Theory of directional pulse propagation

P. Kinsler, S. B. P. Radnor, and G. H. C. New
Department of Physics, Imperial College London, Prince Consort Road, London SW7 2BW, United Kingdom
(Received 5 August 2005; revised manuscript received 30 September 2005; published 13 December 2005)

We construct combined electric and magnetic field variables which independently represent energy flows in the forward and backward directions, respectively, and use these to reformulate Maxwell's equations. These variables enable us to not only judge the effect and significance of backward-traveling field components, but also to discard them when appropriate. They thereby have the potential to simplify numerical simulations, leading to potential speed gains of up to 100% over standard finite difference time-domain (FDTD) or pseudospectral spatial-domain (PSSD) simulations. We present results for various illustrative situations, including an example application to second harmonic generation in periodically poled lithium niobate. These field variables are also used to derive both envelope equations useful for narrow-band pulse propagation, and a second order wave equation. Alternative definitions are also presented.

DOI: 10.1103/PhysRevA.72.063807 PACS number(s): 42.65.Re, 42.25.Bs, 42.65.Ky

I. INTRODUCTION

We introduce electro-magnetic field variables $\mathbf{G}^{\pm}$ that are designed to have directional characteristics. These variables have the potential to speed up numerical simulations, while providing valuable insight into the process of optical pulse propagation at the same time. Simple plane-polarized versions of $\mathbf{G}^{\pm}$ for a dispersionless medium were originally proposed by Fleck at the beginning of Ref. [1], although he did not use them in the rest of the paper. In the generalized form defined below, it is possible to use them to advantage in practical situations. We note that a different approach to directional pulse propagation based on projection operators was proposed by Kolesik *et al.* [2,3]; there is also the recent work of Ferrando *et al.* [4] based on a second order wave equation.

The essential characteristic of $\mathbf{G}^{+}$ and $\mathbf{G}^{-}$ is that they represent energy fluxes directed in the forward and backward directions, respectively. This implies that $\mathbf{G}^{+}$ is the appropriate variable to use in situations where pulses are traveling only in the forward direction. Indeed, as we will explain, optimal construction of $\mathbf{G}^{+}$ makes $\mathbf{G}^{-}$ negligible under these circumstances, and the computational effort can then be halved by neglecting $\mathbf{G}^{-}$ altogether.

If we apply a z-propagated pseudospectral spatial-domain (PSSD) algorithm [5], we also gain a fast and flexible treatment of dispersion and nonlinear effects, which significantly outperforms standard finite difference time-domain (FDTD) methods [6,7]. Further, since many authors (including the recent [3]) assume that the backward field is negligible in any case, the explicit appearance of $\mathbf{G}^{-}$ within our formalism provides a direct test of the validity of this assumption. A further advantage of $\mathbf{G}^{\pm}$ is that it is as easy to include magneto-optic effects as electro-optic effects such as dispersion and nonlinearity. It is in situations involving both electro- and magneto-optic effects where we achieve the greatest computational speed increase—potentially up to 100% faster. Moreover, even if one chooses to propagate an optical pulse using E and H, it is still easy to analyze its directional characteristic by constructing $\mathbf{G}^{\pm}$ after the event.

After reviewing Fleck's original form of the $\mathbf{G}^{\pm}$ variables at the start of Sec. II, we proceed to discuss how to represent the permittivity and permeability of the medium; this is a crucial step in the optimal construction of $\mathbf{G}^{\pm}$ in a generalized form. The treatment of nonlinearities and the calculation of energy and flux are also covered.

In Sec. III, we derive a first-order wave equation, both in a form that is fully equivalent to Maxwell's equations, and in a more useful one that is applicable in the transverse field limit. In Sec. IV, we demonstrate a simple procedure for the numerical implementation of $\mathbf{G}^{\pm}$ simulations; techniques for specifying initial conditions and for handling dispersion and nonlinear effects are examined in detail. We take as an example the case of second harmonic generation in periodically poled lithium niobate, to demonstrate that our method can be applied to practical as well as illustrative simulations. In all cases, we retain both $\mathbf{G}^{+}$ and $\mathbf{G}^{-}$, but show that with optimal construction, $\mathbf{G}^{-}$ can be made negligible.

In Sec. V we derive a propagation equation for envelopes based on $\mathbf{G}^{\pm}$; in Sec. VI we develop a second order wave equation; and in Sec. VII we propose alternative definitions for field variables with directional properties. Finally, in Sec. VIII, we present our conclusions.

II. DEFINITIONS

For plane-polarized fields, propagating in the z direction in a dispersionless medium, Fleck defined the direction field variables

$$G^{\pm} = \sqrt{\epsilon} E_x \pm \sqrt{\mu} H_y. \tag{1}$$

Their directional properties are apparent from the form of the Poynting vector

$$S = E_x H_y = \frac{1}{4\sqrt{\epsilon\mu}} [G^{+2} - G^{-2}], \tag{2}$$

which shows that G^{+} and G^{-} are associated with positive and negative energy flux, respectively. Unfortunately, if Eq. (1) is used to describe a forward-propagating pulse in a *dispersive* medium, it will contain significant contributions from both G^{+} and G^{-}. We, therefore, need to generalize the construction in order to make the concept useful in practical situations.

A. Medium parameters

The definitions of $G^{\pm}$ (and their generalized vector counterparts $\mathbf{G}^{\pm}$, introduced below) depend on the properties of the propagation medium through the permittivity ϵ and permeability μ. In principle it would be attractive to define $\mathbf{G}^{\pm}$ using the exact values of ϵ,μ (including the nonlinearity), but this is usually impractical, and we will instead use "reference" values ϵ_r,μ_r, chosen to be as close as practicable to the true medium properties, typically by including all the dispersive properties.

In the frequency domain (indicated by tildes), we write

$$\tilde{\epsilon} = \tilde{\epsilon}_r(\omega) + \tilde{\epsilon}_c(\omega) = \tilde{\alpha}_r^2(\omega) + \tilde{\alpha}_r(\omega)\tilde{\alpha}_c(\omega), \tag{3}$$

$$\tilde{\mu} = \tilde{\mu}_r(\omega) + \tilde{\mu}_c(\omega) = \tilde{\beta}_r^2(\omega) + \tilde{\beta}_r(\omega)\tilde{\beta}_c(\omega), \tag{4}$$

where the correction parameters $\tilde{\epsilon}_c$ and $\tilde{\mu}_c$ represent the discrepancy between the true values and the reference. The smaller these correction terms are, the better the match, and the more likely it is that a description involving only G^{+} will suffice. Note that since the definitions of $G^{\pm}$ depend on the square roots of $\tilde{\epsilon}$ and $\tilde{\mu}$, we introduce the $\tilde{\alpha}$ and $\tilde{\beta}$ parameters, which will feature prominently (along with their time domain counterparts α,β), in the generalized definitions of $\mathbf{G}^{\pm}$ that follow.

By using these frequency dependent parameters in the generalized definitions of $G^{\pm}$, we are able to propagate pulses using only the G^{+} variable, a gain in both mathematical simplicity and computational speed.

B. $\mathbf{G}^{\pm}$ variables

The generalized definitions of the $\mathbf{G}^{\pm}$ variables in the frequency and time domains are

$$\mathbf{G}^{\pm}(\omega) = \tilde{\alpha}_r(\omega)\mathbf{E}(\omega) \pm \mathbf{u} \times \tilde{\beta}_r(\omega)\mathbf{H}(\omega), \tag{5}$$

$$G^{\circ}(\omega) = \mathbf{u} \cdot [\tilde{\beta}_r(\omega)\mathbf{H}(\omega)]; \tag{6}$$

$$\text{or } \mathbf{G}^{\pm}(t) = \alpha_r(t) * \mathbf{E}(t) \pm \mathbf{u} \times \beta_r(t) * \mathbf{H}(t), \tag{7}$$

$$G^{\circ}(t) = \mathbf{u} \cdot [\tilde{\beta}_r(t) * \mathbf{H}(t)], \tag{8}$$

where $\mathbf{u}$ is the unit vector in the direction of propagation, and $\alpha_r(t)$ and $\beta_r(t)$ are the (inverse) Fourier transformed versions of $\tilde{\alpha}_r(\omega)$ and $\tilde{\beta}_r(\omega)$. The symbol "$*$" is used to denote a convolution: $a*b=\int a(t-t')b(t)dt'$. The variable G° involves the longitudinal part of the magnetic field, which is eliminated in the $\mathbf{u}\times\mathbf{H}$ operation in Eq. (5). Although we will generally make a transverse approximation in which $G^{\circ}=0$ and $\mathbf{u}\cdot\mathbf{G}^{\pm}=0$, we retain the longitudinal parts of the field to ensure a complete description. To avoid cluttering the notation, we do not apply tildes to the spectral forms of the field quantities $\mathbf{G}^{\pm},G^{\circ},\mathbf{E},\mathbf{H}$, and rely instead on the arguments (t or ω) or the context, to distinguish between domains.

Inverting Eq. (5) gives the following expressions for the electric and magnetic fields as a function of $\mathbf{G}^{\pm}$ and G°

$$\mathbf{E}(\omega) = \frac{1}{2\tilde{\alpha}_r(\omega)}[\mathbf{G}^{+}(\omega) + \mathbf{G}^{-}(\omega)], \tag{9}$$

$$\mathbf{H}(\omega) = \frac{1}{2\tilde{\beta}_r(\omega)}\mathbf{u} \times [\mathbf{G}^{+}(\omega) - \mathbf{G}^{-}(\omega)] + \frac{\mathbf{u}G^{\circ}(\omega)}{\tilde{\beta}_r(\omega)}. \tag{10}$$

The divergence of $\mathbf{G}^{\pm}$, allowing for both charge density ρ and current density $\mathbf{J}$, is

$$\nabla \cdot \mathbf{G}^{\pm} = \frac{\tilde{\alpha}_r}{\tilde{\alpha}^2}\rho \pm \frac{\imath\omega}{2}\frac{\tilde{\alpha}^2}{\tilde{\alpha}_r}\tilde{\beta}_r\mathbf{u} \cdot (\mathbf{G}^{+} + \mathbf{G}^{-}) \mp \tilde{\beta}_r\mathbf{u} \cdot \mathbf{J}. \tag{11}$$

We note that this is zero when the ρ and $\mathbf{J}$ are zero, as long as there is no longitudinal electric field.

Different choices of $\tilde{\epsilon}_r,\tilde{\mu}_r$ produce different $\mathbf{G}^{\pm}$ pairs. While using the true values to describe a forward propagating pulse results in $\mathbf{G}^{-}=0$, any other choice of reference will produce a nonzero $\mathbf{G}^{-}$ component that co-propagates with $\mathbf{G}^{+}$. Note that this $\mathbf{G}^{-}$ still has an energy flux directed in the reverse direction ($-\mathbf{u}$), but travels forwards with the $\mathbf{G}^{+}$ with which it is tightly coupled.

We will almost always choose $\tilde{\epsilon}_r,\tilde{\mu}_r$ to include the entire linear dispersion of the medium. We exclude the nonlinearity because it removes the ability to reconstruct $\mathbf{E},\mathbf{H}$ fields uniquely from the $\mathbf{G}^{\pm}$, as can be seen from Eqs. (5), (7), (9), and (10), which will become nonlinear in $\mathbf{E}$ and $\mathbf{H}$.

The vectorized definitions of $\mathbf{G}^{\pm}$ accommodate any polarization of the E and H fields. For propagation along the z axis, the x component of $\mathbf{G}^{\pm}$ ($G_x^{\pm}$) will contain E_x and H_y; and similarly $G_y^{\pm}$, will contain E_y and H_x. It is then a simple matter to see how linearly or circularly polarized $\mathbf{E}$ and $\mathbf{H}$ fields can be represented in terms of $\mathbf{G}^{\pm}$. The definitions are also easily generalized to include birefringent media, provided the propagation direction and transverse coordinate axes are such that ϵ_r and μ_r become diagonal matrices.

Finally, note that $\mathbf{G}^{\pm}$ bear some resemblance to Beltrami variables (see, e.g., Refs. [8–10]) which are defined as $\mathbf{Q}=\sqrt{\epsilon}\mathbf{E}+\imath\sqrt{\mu}\mathbf{H}$; but they differ in two important respects. First, a given Beltrami $\mathbf{Q}$ defines $\mathbf{E}$ and $\mathbf{H}$ uniquely, whereas both $\mathbf{G}^{+}$ and $\mathbf{G}^{-}$ are needed to do the same. Secondly, $\mathbf{Q}$ does not assume any preferred direction, whereas the $\mathbf{G}^{\pm}$ variables include the direction $\mathbf{u}$ in their definition. Further, Beltrami variables are not defined using the full time (or frequency) dependence of ϵ,μ as we use for $\mathbf{G}^{\pm}$ in Eqs. (5) and (7), although presumably this would be possible.

C. Nonlinearities

Since it is usually impractical to include nonlinearities in the reference parameters, these will normally appear in the correction terms ϵ_c,μ_c. As an example, consider a nth order (electric) nonlinearity, in which case $\epsilon_c(t)=\chi^{(n)}(t)*E(t)^{n-1}$, and

$$\tilde{\alpha}_c(\omega) = [\tilde{\alpha}_r(\omega)]^{-1}\mathcal{F}[\chi^{(n)}(t) * E(t)^{n-1}], \tag{12}$$

$$\alpha_c(t) = \mathcal{F}^{-1}\{[\tilde{\alpha}_r(\omega)]^{-1}\tilde{\chi}^{(n)}(\omega)\mathcal{F}[E(t)^{n-1}]\}, \tag{13}$$

where $\mathcal{F}[\ldots]$ is the Fourier transform (FT) from time to frequency, and $E(t)$ can be found from Eq. (9). If the reference parameters $\tilde{\alpha}_r$ contain dispersion (which will be the typical case), we can see from Eq. (12) that this will make $\tilde{\alpha}_c(\omega)$ dispersive even if $\chi^{(n)}$ is instantaneous. In the case of an

instantaneous nonlinearity, this adds more computational work (an extra two FTs), although for noninstantaneous ones we needed the FTs anyway. If the nonlinearity is instantaneous *and* the reference parameters are nondispersive, we have simply $\alpha_c^{NL}(t)=\alpha_r^{-n}\cdot\chi^{(n)}\cdot 2^{-n+1}[G^+ + G^-]^{n-1}$.

D. Energy and flux

The $\mathbf{G}^{\pm}$ are intrinsically directional and do not rely on a carrier wave to impart their directionality. This becomes clear when the Poynting vector is expressed in terms of $\mathbf{G}^{\pm}$. For transverse fields and dispersive reference parameters, we obtain

$$\mathbf{S}=\mathbf{E}\times\mathbf{H} \tag{14}$$

$$\mathbf{S}=\tfrac{1}{4}[(\mathcal{F}^{-1}[\tilde{\alpha}_r^{-1}]*\mathbf{G}^+)\cdot(\mathcal{F}^{-1}[\tilde{\beta}_r^{-1}]*\mathbf{G}^+) - (\mathcal{F}^{-1}[\tilde{\alpha}_r^{-1}]*\mathbf{G}^-)\cdot(\mathcal{F}^{-1}[\tilde{\beta}_r^{-1}]*\mathbf{G}^-)]\mathbf{u}. \tag{15}$$

For dispersionless reference parameters, this becomes simply

$$\mathbf{S}=\frac{1}{4\sqrt{\epsilon_r\mu_r}}[\mathbf{G}^+\cdot\mathbf{G}^+-\mathbf{G}^-\cdot\mathbf{G}^-]\mathbf{u}. \tag{16}$$

Since both the $\mathbf{G}^{\pm}\cdot\mathbf{G}^{\pm}$ terms are real and positive, we see that $\mathbf{G}^+$ and $\mathbf{G}^-$ contribute positive and negative energy fluxes, respectively. This leads to the simple interpretation that for particular $\mathbf{E}$ and $\mathbf{H}$ fields, $\mathbf{G}^+$ corresponds to the energy flux directed forward (along $\mathbf{u}$), and $\mathbf{G}^-$ to flux directed backward. The need for this distinction between the direction of the flux due to a $\mathbf{G}^{\pm}$ field, and its direction of travel has already arisen in Sec. II B above.

We can also calculate the energy density of the EM field, $\mathcal{U}(t)=\frac{1}{2}\epsilon*\mathbf{E}(t)\cdot\mathbf{E}(t)+\frac{1}{2}\mu*\mathbf{H}(t)\cdot\mathbf{H}(t)$. For transverse fields and a nondispersive reference, while still allowing for medium dispersion, the energy density in terms of $\mathbf{G}^{\pm}$ is

$$\mathcal{U}=\frac{1}{8}\left(\left[\frac{\epsilon}{\epsilon_r}+\frac{\mu}{\mu_r}\right]*\mathbf{G}^+\right)\cdot\mathbf{G}^+ +\frac{1}{8}\left(\left[\frac{\epsilon}{\epsilon_r}+\frac{\mu}{\mu_r}\right]*\mathbf{G}^-\right)\cdot\mathbf{G}^- +\frac{1}{8}\left(\left[\frac{\epsilon}{\epsilon_r}-\frac{\mu}{\mu_r}\right]*\mathbf{G}^+\right)\cdot\mathbf{G}^- +\frac{1}{8}\left(\left[\frac{\epsilon}{\epsilon_r}-\frac{\mu}{\mu_r}\right]*\mathbf{G}^-\right)\cdot\mathbf{G}^+. \tag{17}$$

Notice the cross terms, which appear whenever there is a mismatch between the reference and medium parameters. These occur because of the interference between the $\mathbf{G}^+$ and $\mathbf{G}^-$ contributions to the field.

For a dispersive reference, the relevant formulas for $\mathbf{S}$ and $\mathcal{U}$ are relatively complicated because of the appearance of cross terms and/or convolutions. However, this should not produce a significant overhead in numerical simulations because the code will be switching between time and frequency domains at each step, allowing $\mathbf{S}$ and $\mathcal{U}$ to be calculated in whatever way is most efficient.

E. Co-moving frame

We now consider using a moving reference frame. This is particularly useful in a space-propagated model where the pulse is held as a function of time, since it will stay nearly centered when propagating forwards. A simple choice of frame speed might be the phase velocity at the center frequency of the pulse, which minimizes the motion of the carrier-like oscillations; however, the pulse as a whole will move within the frame because of its different group velocity. The frame translation for a speed $c_f=1/\alpha_f\beta_f$ is

$$t'=t-\gamma/c_f \tag{18}$$

$$\mathbf{r}'=\mathbf{r}, \tag{19}$$

where γ is the distance traveled in the direction of $\mathbf{u}$. Thus

$$\partial_t=\partial_{t'}, \tag{20}$$

$$\nabla=\nabla'-\frac{\mathbf{u}}{c_f}\partial_t. \tag{21}$$

In vector calculations, we need to know how this frame translation transforms the curl and divergence operations. The divergence is a straightforward consequence of Eq. (21), and the curl of an arbitrary vector $\mathbf{Q}$ transforms to

$$\nabla\times\mathbf{Q}=\nabla'\times\mathbf{Q}-\alpha_f\beta_f\mathbf{u}\times\partial_t Q. \tag{22}$$

The ratio of the reference speed (the phase velocity in the reference "medium" described by ϵ_r,μ_r) and frame speeds is

$$\xi=\alpha_f\beta_f/\alpha_r\beta_r. \tag{23}$$

If we choose to give α_f and β_f a frequency dependence, we have defined a "dispersive frame," where different frequency components travel at different speeds. In such a frame, any matching dispersive evolution (i.e., where $\alpha_f=\alpha_r$ and $\beta_f=\beta_r$) results in no change to the pulse profile. However, at the end of the simulation, we need to transform from the dispersive frame back into a normal (nondispersive) laboratory frame. Moreover, using a dispersive frame can give rise to numerical stability problems.

III. FIRST-ORDER WAVE EQUATION

We now derive a set of first-order differential equations for the forward and backward directed fields $\mathbf{G}^{\pm}$, and use the moving frame set out above in Eqs. (21) and (22). We assume that the medium is continuous, so that $\partial_z\epsilon=\partial_z\mu=0$, where $\partial_q\equiv d/dq$. This does not impose a significant restriction in practice, since a simulation propagated forwards in space can easily handle interfaces between different media.

A. Derivation

For a vector derivation of propagation equations for $\mathbf{G}^{\pm}$, we start with the two relevant (source free) Maxwell's equations. Writing them in frequency space, with $\tilde{\alpha}^2=\tilde{\epsilon}$ and $\tilde{\beta}^2=\tilde{\mu}$; and taking the cross product of $\mathbf{u}$ and the $\nabla\times\mathbf{H}$ equation yields

$$\mathbf{u}\times(\nabla\times\mathbf{H})=-\imath\omega\tilde{\alpha}^2\mathbf{u}\times\mathbf{E}, \tag{24}$$

$$\nabla \times \mathbf{E} = +\imath\omega\tilde{\beta}^2\mathbf{H}. \tag{25}$$

Multiplying, respectively, by $\tilde{\beta}_r$ and $\tilde{\alpha}_r$ and taking sums and differences leads to

$$\nabla \times \tilde{\alpha}_r\mathbf{E} \pm \mathbf{u} \times (\nabla \times \tilde{\beta}_r\mathbf{H}) = +\imath\omega\tilde{\alpha}_r\tilde{\beta}^2\mathbf{H} \mp \imath\omega\tilde{\beta}_r\tilde{\alpha}^2\mathbf{u} \times \mathbf{E}. \tag{26}$$

Noting the similarities between this and Eq. (7), we now reorganize using standard vector identities for $\nabla \times (\mathbf{A} \times \mathbf{B})$ and $\mathbf{u} \times (\mathbf{u} \times \mathbf{A})$. Finally, we arrive at a curl equation for $\mathbf{G}^{\pm}$, namely

$$\nabla \times \mathbf{G}^{\pm} = \mp \imath\omega\{\tilde{\beta}_r\tilde{\alpha}^2\mathbf{u} \times \mathbf{E} \pm \tilde{\alpha}_r\tilde{\beta}^2\mathbf{u} \times [\mathbf{u} \times \mathbf{H}]\} + \imath\omega\tilde{\alpha}_r\tilde{\beta}^2\mathbf{u}G^{\circ} \mp \nabla G^{\circ}. \tag{27}$$

We now separate the correction components (depending on $\tilde{\alpha}_c$, $\tilde{\beta}_c$) from the reference components (depending on $\tilde{\alpha}_r$, $\tilde{\beta}_r$), and substitute expressions containing $\mathbf{G}^{\pm}$ G° by referring to Eqs. (9) and (10). We also note that the terms involving $\mathbf{G}^{\pm}$ decouple from those involving G°. Hence

$$\nabla \times \mathbf{G}^{\pm} = \mp \imath\omega\tilde{\alpha}_r\tilde{\beta}_r\mathbf{u} \times \mathbf{G}^{\pm} \mp \frac{\imath\omega\tilde{\alpha}_c\tilde{\beta}_r}{2}\mathbf{u} \times [\mathbf{G}^{+} + \mathbf{G}^{-}] - \frac{\imath\omega\tilde{\alpha}_r\tilde{\beta}_c}{2}\mathbf{u} \times [\mathbf{G}^{+} - \mathbf{G}^{-}], \tag{28}$$

$$\nabla G^{\circ} = \pm\imath\omega\tilde{\alpha}_r\tilde{\beta}_r\mathbf{u}G^{\circ} \pm \imath\omega\tilde{\alpha}_r\tilde{\beta}_c\mathbf{u}G^{\circ}. \tag{29}$$

For media whose magnetic behavior is matched perfectly by the reference parameters (i.e., $\tilde{\beta}_c = 0$), this simplifies to

$$\nabla \times \mathbf{G}^{\pm} = \mp \imath\omega\tilde{\alpha}_r\tilde{\beta}_r\mathbf{u} \times \mathbf{G}^{\pm} \mp \frac{\imath\omega\tilde{\alpha}_c\tilde{\beta}_r}{2}\mathbf{u} \times [\mathbf{G}^{+} + \mathbf{G}^{-}], \tag{30}$$

$$\nabla G^{\circ} = \pm\imath\omega\tilde{\alpha}_r\tilde{\beta}_r\mathbf{u}G^{\circ}. \tag{31}$$

For propagation along the z axis, in the plane polarized (E_x, H_y) limit, the curl becomes ∂_z, and $\mathbf{G}^{\pm}$ is replaced with $G_x^{\pm}$. In the transverse field case, Eq. (31) [or (29)] can be ignored.

The equations above are written to suggest a spatially directed propagation (along $\mathbf{u}$), and indeed are most straightforwardly solved that way. However, a simple rearrangement of the terms leads to a t-directed propagation model, although, in its present form, the time-like evolution of Eq. (30) is obscured. While t-directed propagation has some advantages, it makes the treatment of dispersion and other time-memory effects more demanding, as discussed by Kolesik and Moloney [3] and Tyrrell *et al.* [5].

In the time domain, Eq. (30) becomes

$$\nabla \times \mathbf{G}^{\pm} = \pm\partial_t[(\alpha_r * \beta_r) * (\mathbf{u} \times \mathbf{G}^{\pm})] \pm \partial_t\left[\left(\frac{\alpha_c * \beta_r}{2}\right) * (\mathbf{u} \times [\mathbf{G}^{+} + \mathbf{G}^{-}])\right]. \tag{32}$$

Note that reversing the direction of propagation by changing $\mathbf{u}$ to $-\mathbf{u}$ reverses the roles of $\mathbf{G}^{+}$ and $\mathbf{G}^{-}$.

B. Longitudinal E

In the same way that the construction of $\mathbf{G}^{\pm}$ ignores the contribution from $\mathbf{H}$ along the propagation vector $\mathbf{u}$, and forces us to define G°, Eq. (24) ignores information about the time-evolution of the longitudinal part of $\mathbf{E}$. We can rectify this by using $\nabla \cdot (\mathbf{u} \times \mathbf{H}) = \mathbf{u} \cdot (\nabla \times \mathbf{H})$, to get

$$\tilde{\alpha}_r \nabla \cdot [\mathbf{G}^{+} - \mathbf{G}^{-}] = -\imath\omega\tilde{\alpha}^2\tilde{\beta}_r\mathbf{u} \cdot [\mathbf{G}^{+} + \mathbf{G}^{-}]. \tag{33}$$

This is the difference of the source-free divergences for $\mathbf{G}^{\pm}$ calculated in Eq. (11). Thus Eqs. (28), (29), and (33) provide another way of solving the complete set of source-free Maxwell's equations using an alternative basis. Clearly, however, our basis of $\mathbf{G}^{\pm}$, G° is most useful for fields propagating mainly along one axis (i.e., $\mathbf{u}$), particularly in the limit of transverse fields, where only Eq. (28) needs to be solved.

C. Co-moving frame

We can transform Eq. (28) directly into a moving frame using Eq. (22), which gives

$$\nabla' \times \mathbf{G}^{\pm} = \mp\imath\omega\alpha_r\beta_r(1 \mp \xi)\mathbf{u} \times \mathbf{G}^{\pm} \mp \frac{\imath\omega\alpha_c\beta_r}{2}\mathbf{u} \times [\mathbf{G}^{+} + \mathbf{G}^{-}] - \frac{\imath\omega\alpha_r\beta_c}{2}\mathbf{u} \times [\mathbf{G}^{+} - \mathbf{G}^{-}]. \tag{34}$$

Here we have not shown the transformed (nontransverse) Eqs. (29) and (33) in the interest of brevity, but they are easy to calculate if needed.

One nice property of this equation is that matching the frame velocity to the phase velocity causes the carrier-like oscillations in the forward traveling fields G^{+} to freeze in place, leaving only the evolution due to the correction terms. If we are prepared to make the common assumption of only forward-traveling pulses, we will have managed to greatly reduce the rate of change of the fields. This in turn will allow coarser numerical resolutions to be employed in numerical simulations, leading to significant speed advantages over and above those obtained by assuming $G^{-} = 0$.

D. Time vs space propagation

In FDTD solutions of Maxwell's equations, optical pulses travel either forwards or backwards in space as they propagate (or march) forward with time. However, most nonlinear optical simulations are done in a space-propagated picture; with the consequence that optical pulses travel either forwards or backwards in *time* as the calculations propagate (march) through space.

Since we follow the space-propagated picture, the pulse traveling forward in time will be described by G^{+}, and the one traveling backward by G^{-}.

Note that any backward traveling pulse in a z-propagated picture is traveling backwards in time while propagating forwards in space. Although at first this might seem noncausal,

it is in fact the way that the simulation represents a pulse which we would normally describe as propagating backwards (i.e., in the direction $-\mathbf{u}$). This is clear from the wave equations; swapping the sign of the propagation direction $\mathbf{u}$ swaps the behavior of $\mathbf{G}^+$ and $\mathbf{G}^-$.

E. Decoupled wave equations

We can make the most of our approach by decoupling $\mathbf{G}^+$ from $\mathbf{G}^-$, enabling the two first-order coupled Maxwell's Eqs. (24) and (25) or $\mathbf{G}^\pm$ Eqs. (28) [or co-moving form Eq. (34)] to be reduced to two uncoupled first-order equations. The equation describing propagation in the "uninteresting" direction can then be discarded, leaving one first-order equation where there were originally two.

This step requires an approximation, although since we can perfectly match the reference parameters (α_r, β_r) to the material dispersion, it is not a very stringent one. Since the correction parameters α_c, β_c depend only on nonlinear effects, they will in general be small, keeping cross coupling between $\mathbf{G}^+$ and $\mathbf{G}^-$ minimal. Further, while the $\mathbf{G}^+$ field will rotate forwards according to its wavevector (i.e., $e^{+\imath kz}$, with $k=\alpha_r\beta_r\omega$), the $\mathbf{G}^-$ field will rotate backwards at the same rate (i.e., at $e^{-\imath kz}$). This means the correction terms for $\mathbf{G}^+$ will contain both an in-sync component from $\mathbf{G}^+$, and a component from $\mathbf{G}^-$ with a large detuning. Since this detuning (amounting to $e^{-2\imath kz}$) will usually be large compared to the spatial bandwidth of the pulse, we can apply a rotating wave approximation and average the $\mathbf{G}^-$ contribution to zero. After applying the same steps to the $\mathbf{G}^-$ equation as well, Eq. (28) becomes

$$\nabla\times\mathbf{G}^\pm = \mp\imath\omega\tilde{\alpha}_r\tilde{\beta}_r\mathbf{u}\times\mathbf{G}^\pm \mp \frac{\imath\omega\tilde{\alpha}_c\tilde{\beta}_r}{2}\mathbf{u}\times\mathbf{G}^\pm \mp \frac{\imath\omega\tilde{\alpha}_r\tilde{\beta}_c}{2}\mathbf{u}\times\mathbf{G}^\pm, \tag{35}$$

IV. SIMULATING $G^\pm$

We now examine the procedure needed to simulate wave propagation using the $G^\pm$ variables. This will clarify various practical issues as well as illuminate some of the less-obvious features of our approach. We consider a plane-polarized EM wave propagating along z in a nonmagnetic medium with dispersion and a weak nonlinearity. Since our aim is to explain the fundamental principles of the use of $G^\pm$ variables, we first present a number of simple examples.

Our numerical simulations of the $\mathrm{G}^\pm$ wave equations are implemented by straightforward adaption of the PSSD technique [5]. In PSSD, fields are stored as functions of time, and fast Fourier transforms (FFTs) are used to convert to the frequency domain for the calculation of pseudospectral derivatives and the effects of dispersion. This technique allows the simple application of arbitrary dispersion, which becomes a simple multiplication in frequency space. Fields are then transformed back to the time domain, where the nonlinear effects are calculated, before propagating the fields forward in space. Computational details, such as how to design the mesh and control the accuracy of the simulations are well known (e.g., the Courant and Nyquist criteria), and can be found in a range of sources (e.g., Refs. [13,14]).

When applied to $\mathrm{G}^\pm$ fields, the basic spatially propagated PSSD algorithm does not change, but the wave equation to be solved is now Eq. (30) instead of Maxwell's equations. This means that the full flexibility of PSSD is harnessed with the advantages of $\mathrm{G}^\pm$ fields to give a powerful and efficient combination.

A. Simulation speed

The computational speed of any PSSD-type propagation depends primarily on the time spent doing FTs. In the PSSD technique described in [5], five FTs are used, two forward and back pairs, and one (forward only) to calculate the derivative of the electric displacement D. If magnetic dispersion were present, PSSD would require an extra FT for the magnetic induction B, making six FTs in all.

In contrast, a G^+ simulation requires only three FTs. This comprises two forward FTs which are used to calculate the derivative for the dispersion and nonlinearity, and one backward FT is used to change back into the time domain; the two derivatives are combined in the frequency domain where the problem becomes linear. Such a simulation will, therefore, run 67% faster than the corresponding E and H PSSD algorithm; or 100% if there is also magnetic dispersion.

To include both G^+ and G^- would require six FTs; one more than the usual PSSD case, but the same if magnetic dispersion needs to be included.

B. Implementation

As a first step, we divide the total permittivity into three: A reference component with constant permittivity $\tilde{\epsilon}_r$, a linear dispersion correction $\tilde{\epsilon}_c^D(\omega)$, and an instantaneous nonlinearity $\tilde{\epsilon}_c^{NL}$; the permeability has the vacuum value μ_0. The medium properties can, therefore, be represented in the following fashion

$$\tilde{\epsilon}(\omega) = \tilde{\epsilon}_r + \tilde{\epsilon}_c^D(\omega) + \tilde{\epsilon}_c^{NL} \tag{36}$$

$$= \tilde{\alpha}_r^2 + \tilde{\alpha}_r\tilde{\alpha}_c^D(\omega) + \tilde{\alpha}_r\tilde{\alpha}_c^{NL} \tag{37}$$

This particular breakdown of $\tilde{\epsilon}$ is for illustrative purposes only; in practice, we would choose a dispersive reference and try to leave only nonlinear terms in the correction parameters (i.e., use $\tilde{\epsilon}(\omega)=\tilde{\epsilon}_r(\omega)+\tilde{\epsilon}_c^{NL}$). We might also regroup various terms to optimise the numerical performance.

The first-order evolution equation, specialized from Eq. (30), is

$$\partial_z G_x^\pm = \mp\imath\omega\tilde{\alpha}_r\tilde{\beta}_r(1\mp\xi)G_x^\pm \mp \frac{\imath\omega\tilde{\alpha}_c^D\tilde{\beta}_r}{2}[G_x^+ + G_x^-] \mp \frac{\imath\omega\tilde{\alpha}_c^{NL}\tilde{\beta}_r}{2}[G_x^+ + G_x^-]. \tag{38}$$

where the RHS contains respectively a reference carrier term ($\propto \tilde{\alpha}_r$), a linear dispersion term ($\propto\tilde{\alpha}_c^D$), and a nonlinear po-

larization term ($\propto \tilde{\alpha}_c^{NL}$). We integrate forward in z using a split-step method, where each term is integrated through δz in sequence. This procedure is accurate to first order, so we need to ensure δz is sufficiently small.

In this simple case, the reference term merely applies a complex rotation to the field in frequency space represented by

$$G_{x1}^{\pm} = G_x^{\pm}(z) \times \exp[\mp \imath\omega\tilde{\alpha}_r\tilde{\beta}_r(1 \mp \xi) \,.\, \delta z]. \tag{39}$$

If the frame velocity is chosen to be the same as the phase velocity given by the reference parameters, the G_x^+ field no longer undergoes any reference evolution as it propagates. This contrasts with the usual approach, which is to match the frame velocity to the group velocity. However, with our choice of reference parameters, the group velocity corrections appear in the second RHS term as part of $\tilde{\alpha}_c^D$. If we were to propagate $G_x^{\pm}$ in a group velocity frame, we would retain part of the reference term, which would then cancel with part of the group velocity contribution from the dispersion term. This could lead to a better overall cancellation, just as in the usual E field approaches. If that were our aim, we could indeed easily rearrange Eq. (38) to incorporate such a cancellation, and then solve the equation appropriately.

The next step is to solve for the linear dispersion $\alpha_c^D = \tilde{\epsilon}_c^D / \alpha_r$. Fortunately, this part of the equation is also easy to solve exactly in the frequency domain, through the operation

$$G_{x2}^{\pm} = G_{x1}^{\pm} \times \exp\left[\mp \imath k G_{x1}^{\pm} \cdot \delta z \mp \frac{\imath\omega\tilde{\epsilon}_c^D(\omega)}{2} \times \sqrt{\frac{\mu_r}{\epsilon_r}}[G_{x1}^+ + G_{x1}^-] \cdot \delta z \right]. \tag{40}$$

Although both reference and dispersion steps can be solved using exponentials, there is an important difference. The reference evolution of G^+ depends only on G^+, whereas the dispersion evolution depends on the sum $G^+ + G^-$, since the dispersion acts on the electric field. In a forward-only approximation where $G^- = 0$, it is trivial to combine these first two steps, as in most approaches to solving for the propagation of optical pulses.

The third and final step is performed by transforming into the time domain and solving for the nth order nonlinear effects. Since the reference α_r, β_r are constants, $\alpha_c^{NL} = \chi^{(n)} E^{n-1} / \alpha_r$, a simple Euler method gives

$$G_x^{\pm}(z + \delta z) = G_{x2}^{\pm} \pm \frac{\chi^{(n)}}{2^n} \sqrt{\frac{\mu_r}{\epsilon_r^{n-1}}} \times \partial_t [G_{x2}^+ + G_{x2}^-]^n \delta z. \tag{41}$$

For a narrow-band field centred at ω_0, the time derivative would be dominated by (and proportional to) ω_0. In most envelope theories we see only this factor ω_0 in the analogous expression; although correction terms exist for wider-band fields [11,12].

C. Initial conditions: Matching a pulse to the medium

Most descriptions of pulse propagation start with initial conditions chosen to represent a pulse traveling forward in the medium. Here we consider how to choose the best initial conditions for $G^{\pm}$ in the case of a pulse traveling *only* in the forward **u** direction. They are based on the best practical parameterization of the medium $\tilde{\epsilon}_i(\omega), \tilde{\mu}_i(\omega)$, which need not be the same as $\tilde{\epsilon}_r$ and $\tilde{\mu}_r$. Assuming only the electric field $E(\omega)$ of the pulse is known, the procedure is:

(1) Choose $\tilde{\epsilon}_i$ and $\tilde{\mu}_i$ to be as close as possible to the actual medium parameters $\tilde{\epsilon}, \tilde{\mu}$. One might even try to put the nonlinear properties into $\tilde{\epsilon}_i$ and $\tilde{\mu}_i$ as well, but only if one can get a solution for steps (2) and (3) below with this added complication.

(2) Calculate $H(\omega)$ corresponding to $E(\omega)$ for a forward traveling pulse, so that a G^- based on $\tilde{\epsilon}_i, \tilde{\mu}_i$ would be zero:

$$H(\omega) = -\sqrt{\frac{\tilde{\epsilon}_i(\omega)}{\tilde{\mu}_i(\omega)}} E(\omega). \tag{42}$$

(3) Calculate an initial $G^{\pm}$ using the chosen reference parameters $\epsilon_r(\omega)$ and $\mu_r(\omega)$, given our initial $E(\omega)$ and $H(\omega)$ fields:

$$G^{\pm} = \left[\sqrt{\tilde{\epsilon}_r(\omega)} \pm \sqrt{\tilde{\mu}_r(\omega)} \sqrt{\frac{\tilde{\epsilon}_i(\omega)}{\tilde{\mu}_i(\omega)}} \right] E(\omega). \tag{43}$$

Note that step (3) is unnecessary if $\tilde{\epsilon}_i = \tilde{\epsilon}_r$ and $\tilde{\mu}_i = \tilde{\mu}_r$.

Notwithstanding step (2), G^- is only eliminated from the simulation if both $\tilde{\epsilon}_i$ and $\tilde{\mu}_i$ are perfect matches to the material parameters. If the $(\tilde{\epsilon}_i, \tilde{\mu}_i)$ values are good, but $(\tilde{\epsilon}_r, \tilde{\mu}_r)$ less so, a weak G^- field will co-propagate *forwards* with G^+, even though the Poynting vector of the G^- is directed backwards. If $(\tilde{\epsilon}_i, \tilde{\mu}_i)$ is a bad match as well, the initial G^- will have a component that *travels* backwards, its magnitude corresponding to that of the reflection between a medium with parameters $(\tilde{\epsilon}_i, \tilde{\mu}_i)$ and one with the actual parameters. Since it is usually possible to include all the linear dispersive properties in $\tilde{\epsilon}_i, \tilde{\mu}_i$, any discrepancy is likely to be due to the nonlinear contribution, and consequently very small.

Figure 1 shows how different choices of reference parameter affect the $G^{\pm}$ fields required to model a simple forward-propagating few-cycle pulse at 500 nm in fused silica. Note that although the $G^{\pm}$ fields in Figs. 1(a) and 1(b) are directly proportional to E and H, in Fig. 1(c), the use of a dispersive reference means that a deconvolution would be needed (if in the time-domain) to transform from $G^{\pm}$ to E and H.

In Fig. 1(a), the mismatch between the reference parameters (with $n=1$) and the actual medium ($n \approx 1.5$ at the 500 nm pulse center wavelength) causes a significant co-propagating G^- component to appear; this is improved in Fig. 1(b) where the reference parameters specify a constant refractive index close to that at the center frequency of the initial pulse. Since the mismatch between the reference and the true material properties is due only to the material dispersion, the initial co-propagating G^- component is smaller in Fig. 1(b) than in Fig. 1(a). The reduction in the size of G^- is rather smaller than might be expected, mainly because although fused silica has a refractive index of about 1.5 at 500 nm, we have used nondispersive reference parameters with a refractive index of 1.5 at all frequencies.

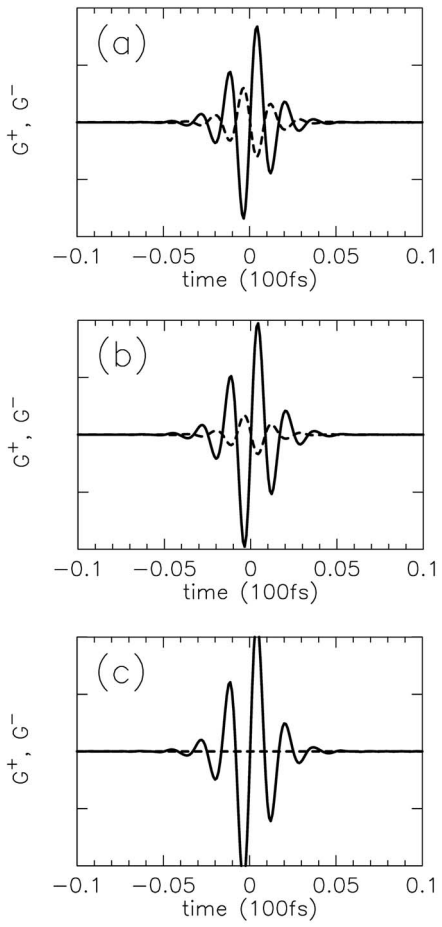

FIG. 1. A 500 nm pulse in fused silica, represented with (a) a vacuum reference, (b) a fixed refractive index reference, (c) a perfectly matched dispersive reference. In all cases the initialization parameters are those that perfectly match the dispersive properties of the medium. Solid line: G^+ field. Dashed line: G^- field.

In Fig. 1(b), although the construction of $G^{\pm}$ has the phase velocity reasonably well matched, the group velocity of the pulse is poorly matched. In addition there is a smaller effect caused by the wide-band nature of the pulse, where the reference parameters are (even) less well matched to frequency components away from the center frequency.

The conclusion is that, for any pulse propagating in a material whose dispersion is not perfectly matched by the reference over the pulse bandwidth, a finite co-propagating G^- will appear. This will be made up of frequency components whose phase velocity in the medium do not match the phase velocity given by the reference. Thus, in typical dispersive media, only very narrow-band pulses result in a negligible G^- for nondispersive reference parameters. However, the mismatch between the reference and the true material properties can be completely removed by using a dispersive reference identical to that of the material being simulated. The results of this are shown in Fig. 1(c), where G^- is identically zero.

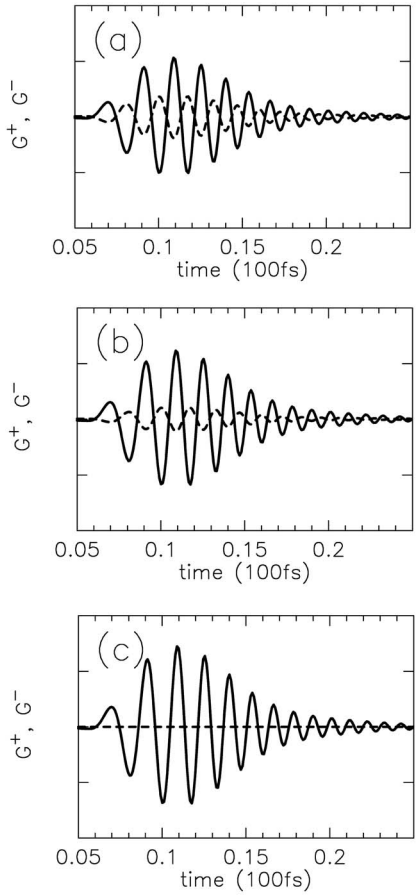

FIG. 2. The same pulse as in Fig. 1, after propagating 15 μm; represented in (a) a vacuum reference, (b) a fixed refractive index reference (c) a perfectly matched dispersive reference. Solid line: G^+ field. Dashed line: G^- field.

D. Dispersive propagation

We now present a variety of numerical results demonstrating pulse propagation in a dispersive medium. We take the medium to have the properties of fused silica, but we do not include nonlinear effects for the moment. Our aim is to give a flavour of what the $G^{\pm}$ fields look like for different reference parameters. The choice of reference is important because, as explained earlier, if the reference is not perfectly matched to the actual medium, a forward traveling pulse will contain a G^- wave co-propagating with the main G^+ component. Usually we will want to choose a reference that makes G^- negligible, so we can save computational effort.

We deliberately choose ultra-short pulses containing only a few optical cycles to demonstrate the flexibility of our method in the short pulse limit.

Figure 2 shows the results for the fields in Fig. 1 after propagating 15 μm in fused silica with the nonlinearity ignored. In all cases, the initial size of G^- is broadly maintained and, in particular, it remains zero when the reference parameters are perfectly matched. Although the $G^{\pm}$ fields in Figs. 2(a) and 2(b) are directly proportional to E and H, in Fig. 2(c), the use of a dispersive reference means that in that case a deconvolution is needed to transform from $G^{\pm}$ to E and H.

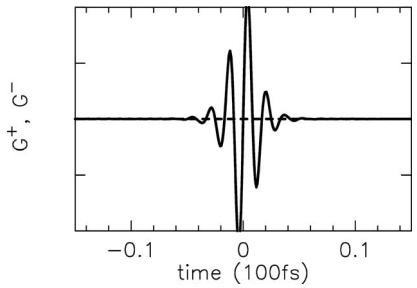

FIG. 3. Simulation results showing $G^{\pm}$ for perfect reference $[\epsilon_r=\epsilon_{\text{silica}}(\omega)]$ and a matched dispersive frame.

We can also consider the effect of neglecting a finite (but significant) G^- field, where the G^+ part of the pulse then undergoes the wrong dispersion. This is because the dispersive correction part [see, e.g., Eq. (38)] depends on $G^+ + G^-$, and thus, without G^-, will be either too big or too small. This problem is avoided by using a dispersive reference identical to that of the material being simulated. The results of this are shown in Fig. 2(c), where G^- is always identically zero and no approximation is necessary to omit G^-.

In Fig. 3 we show the result for a simulation with both a perfectly matched dispersive reference *and* a perfectly matched dispersive frame. Since all the material properties are included in the reference parameters, *and* we pick a frame that exactly matches the propagation, Fig. 3 looks identical to the initial state in Fig. 1(c). We can recover the expected lab-frame final state by transforming Fig. 3 out of its dispersive frame, and so get a graph identical to Fig. 2(c).

The main message from these simulations is that the better matched the reference parameters are to the material parameters, the smaller the co-propagating G^-. For a perfectly matched reference, the co-propagating G^- vanishes. Also, the better matched the frame is to the material parameters, the slower the evolution of the pulse shape. However, we then have to do more work to transform the final state of the pulse (in its moving frame) into the stationary-frame counterpart we would see in the lab—although for a linearly dispersive frame, the transformation is straightforward.

E. Nonlinear propagation

We now demonstrate some simple pulse propagations in nonlinear media. Since neither the initial conditions (determined by ϵ_i, μ_i) nor the reference parameters (determined by ϵ_r, μ_r) include the nonlinearity, the pulse is not perfectly forward propagating, and a small "reflection" occurs as the pulse starts propagating in the nonlinear medium.

Figure 4 shows how pulses similar to those in Fig. 1 look after propagating 10 μm through fused silica. The pulse parameters were adjusted to give a clearer final pulse shape. We see the same pattern as in Figs. 1 and 2, where a weak G^- remains except for perfectly matched reference parameters. Note, however, that the addition of nonlinearity does not cause the size of the G^- field to change significantly during propagation.

We now apply our approach to the practical problem of second harmonic generation in 120 μm of periodically poled lithium niobate. The results are shown on Fig. 5, and agree with the simulations of Tyrrell *et al.* [5].

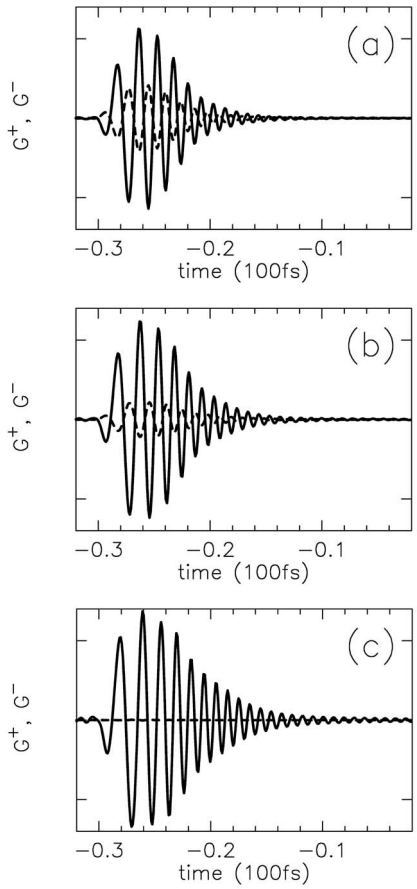

FIG. 4. A similar pulse as above, after propagating 10 μm through fused silica; represented in (a) a vacuum reference, (b) a fixed refractive index reference ($n=1.5$), (c) a perfectly matched dispersive reference. Parameters have been adjusted to give a clearer final pulse shape. Solid line: G^+ field. Dashed line: G^- field.

F. Some remarks on layered media

A complication arises when propagating a pulse through layers of material with significantly different dispersions. Because the $\mathbf{G}^{\pm}$ definitions are carefully constructed to match the propagation medium, $\mathbf{G}^{\pm}$ variables ideal for one layer (and so ensuring $\mathbf{G}^-=0$) will not be ideal for another. This gives us two options: (a) Either retain the $\mathbf{G}^-$ field in the description, or (b) at each layer boundary, switch to a set of $\mathbf{G}^{\pm}$ variables matched to that medium. Option (a) is simpler, but it is not necessarily computationally efficient and leads to complications involving reflections from the interfaces. Option (b) is more efficient computationally when we are only interested in the forward-going pulse, as the effort involved in switching $\mathbf{G}^{\pm}$ definitions is comparable to only a single spatial step in the ongoing propagation calculation.

G. Justifying the forward-only approximation

The ability to accurately incorporate dispersion into our reference permittivity allows great control over the magni-

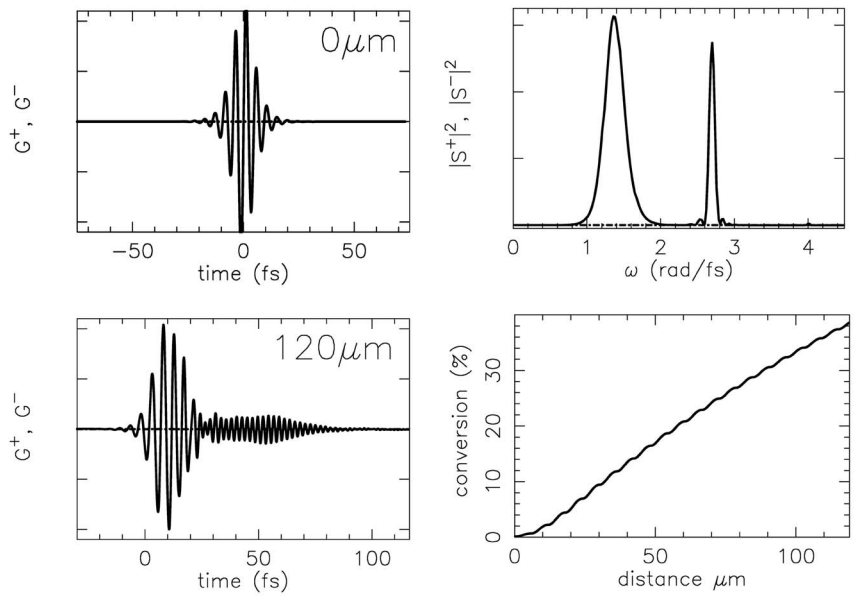

FIG. 5. Second harmonic generation in 120 μm of $LiNO_3$, periodically poled at 6.05 μm. Clockwise from top left: Initial pulse, final pulse, second harmonic power, final pulse spectrum. Solid line: G^+ field. Dot-dashed line: G^- field.

tude of the G^- field. Our tests have shown that we can confidently neglect G^- if our construction of $G^\pm$ accurately includes the medium dispersion, although possible exceptions may occur in cases involving extremely strong nonlinearities.

This can be seen in the case of periodically poled lithium niobate discussed above (see Fig. 5), where the ratio of the G^- to G^+ intensities was $1:10^6$. An even more rigorous test of G^+'s ability to accurately simulate short pulse propagation was our recent study of the effects of dispersion on carrier shocking [15]. Despite the strong nonlinear effects, and significant distortion to the pulse profiles, G^+ simulations consistently produced results in agreement with PSSD—while still only requiring half the computational effort.

The ability to accurately model pulse propagation using *only* G^+ after carefully choosing a reference permittivity clearly justifies neglecting G^-, which in turn simplifies numerical simulations.

V. ENVELOPE PROPAGATION EQUATION

When computing the interaction of narrow-band fields, it is common to remove chosen carrier frequencies, and to evolve the envelopes rather than the complete EM fields. In fact, if sufficient care is taken with the approximations, and the system simulated is well behaved, even quite wide-band pulses can be successfully modeled in this way.

We can use an envelope approach with the $G^\pm$ variables. However, a full model requires four envelopes to describe the $G^\pm$, just as in a complete Maxwell theory where envelopes are needed for both the backward and forward traveling E and H. A full expansion of $G^\pm$ into forward and backward envelopes $G_f^\pm, G_b^\pm$ would be

$$G^\pm(\omega) = \mathcal{G}_f^\pm(\omega \mp \omega_0)e^{\pm \imath kz} + \mathcal{G}_f^{\pm *}(\omega \mp \omega_0)e^{\mp \imath kz} + \mathcal{G}_b^\pm(\omega \mp \omega_0)e^{\pm \imath k_0 z} + \mathcal{G}_b^{\pm *}(\omega \mp \omega_0)e^{\mp \imath k_0 z}, \quad (44)$$

where we have suppressed the z argument on the envelope functions for brevity. Note that the forward-like G^- contribution (i.e., $\mathcal{G}_f^-$) needs a backward-traveling carrier, as otherwise it is not possible to match the reference evolution terms for both $\mathcal{G}_f^+$ and $\mathcal{G}_f^-$. When inserted into the wave equations, this expansion results in a large number of terms, even for the relatively simple case of a third-order nonlinearity. However, we can specialize to the case where only forward-traveling waves are considered, and set $\mathcal{G}_b^\pm = 0$. Since the backward-traveling waves are now eliminated, we can propagate pulses efficiently in a moving frame. This is important, because the backward parts in a moving frame move at *twice* the frame speed. In a full (nonenvelope) simulation, we need somehow to filter out the backward components, as otherwise the hoped-for numerical gains are lost by the fact that a finer z-step is required for accurate integration.

The first-order wave equation for the forward-traveling envelopes defined above is

$$\partial_z \mathcal{G}_f^\pm = \mp \imath(\omega \tilde{\alpha}_r \tilde{\beta}_r - k_0)\mathcal{G}_f^\pm \mp \frac{\imath \omega a_c \tilde{\beta}_r}{2}\{\mathcal{G}_f^\pm + \mathcal{G}_f^{\mp *}\}. \quad (45)$$

Here $a_c + a_c^* = \tilde{\alpha}_c$, which is simple in the case of dispersion but, in the presence of nonlinearity, will be the appropriately carrier-matched, positive frequency part of the permittivity correction parameter.

If $\omega_0 = k_0 c_r$, we have

$$\partial_z \mathcal{G}_f^\pm = \mp \imath \tilde{\alpha}_r \tilde{\beta}_r(\omega - \omega_0)\mathcal{G}_f^\pm \mp \frac{\imath \omega a_c \tilde{\beta}_r}{2}\{\mathcal{G}_f^\pm + \mathcal{G}_f^{\mp *}\}. \quad (46)$$

In a suitable narrow-band limit, we should be able to ignore the first term on the RHS of this equation, leaving the evolution of the envelopes to be controlled solely by the correction term. The description can be easily generalized to cases involving multiple components centred on different carrier frequencies. Note that this is a first-order envelope equation, and, as such, does not require the various extra approximations needed when deriving an envelope propaga-

tion equation from the standard (E field) second order wave equation.

VI. SECOND-ORDER WAVE EQUATION

In Sec. III we derived first-order wave equations for the field variables $\mathbf{G}^{\pm}$. However, since many pulse propagation theories start from a second-order form, we have also derived a second-order propagation equation. We apply the usual restriction to transverse-only fields, and split the medium properties (i.e., the permittivity and permeability) into a reference part (with $c_r = 1/\alpha_r\beta_r$), a linear dispersive part (controlled by α_c^D, β_c^D) and a nonlinear electro-optic polarization part ($\mathbf{P} = \alpha_r \alpha_c^{NL} * \mathbf{E}$). The time-domain wave equation for a nondispersive reference is

$$\nabla^2 \mathbf{G}^{\pm} - \frac{1}{c_r^2}\partial_t^2 \mathbf{G}^{\pm} - \frac{1}{2}\partial_t \left\{ \frac{1}{c_r}\partial_t \mp \mathbf{u} \times \nabla \times \right\} . \{\alpha_c^D * [\mathbf{G}^+ + \mathbf{G}^-] \pm \beta_c^D * [\mathbf{G}^+ - \mathbf{G}^-]\} = + \frac{1}{2\alpha_r}\partial_t \left[\frac{1}{c_r}\partial_t \mp \mathbf{u} \times \nabla \times \right] \mathbf{P}. \quad (47)$$

This is similar to the usual second-order equation for the electric field, but has the addition of a curl operator applied to the dispersion and polarization terms. This second-order wave equation can be solved with the use of an envelope-carrier representation for $\mathbf{G}^{\pm}$, as is often done with the standard equation for the electric field E. Such a derivation can be found in [16], which contains both SVEA and GFEA [12] versions for both E and $G^{\pm}$. The most general form of Eq. (47) appears in [17].

VII. ALTERNATIVE DEFINITIONS

Just as one may decide to propagate the D field instead of the E field, so directional field variables in the style of $\mathbf{G}^{\pm}$ can be defined in a number of ways. Continuing with the pattern of combining transverse field components with a cross product, alternative directional fields are

$$\mathbf{G}'^{\pm} = \mathbf{u} \times \tilde{\alpha}_r \mathbf{E} + \tilde{\beta}_r \mathbf{H}, \quad G'^{\circ} = \mathbf{u} \cdot \tilde{\alpha}_r \mathbf{E}; \quad (48)$$

$$\mathbf{F}^{\pm} = \tilde{\alpha}_r^{-1} \mathbf{D} + \mathbf{u} \times \tilde{\beta}_r^{-1} \mathbf{B}, \quad F^{\circ} = \mathbf{u} \cdot \tilde{\beta}_r^{-1} \mathbf{B}; \quad (49)$$

$$\mathbf{F}'^{\pm} = \mathbf{u} \times \tilde{\alpha}_r^{-1} \mathbf{D} + \tilde{\beta}_r^{-1} \mathbf{B}, \quad F'^{\circ} = \mathbf{u} \cdot \tilde{\alpha}_r^{-1} \mathbf{D}. \quad (50)$$

The $\mathbf{G}^{\pm}$ or $\mathbf{G}'^{\pm}$ variables will best suit problems defined in terms of $\mathbf{E}$ and $\mathbf{H}$; the $\mathbf{G}^{\pm}$ are best suited to electric media, and the $\mathbf{G}'^{\pm}$ to magnetic media. In contrast, the $\mathbf{F}^{\pm}$ or $\mathbf{F}'^{\pm}$ variables are more suited to $\mathbf{D}$ and $\mathbf{B}$. All these definitions can be used to generate wave equations, by a similar procedure to that in Sec. III. A point to note is that if the wave equations are generalized to include source terms, the $\mathbf{G}^{\pm}$ and $\mathbf{G}'^{\pm}$ forms (or $\mathbf{F}^{\pm}$ and $\mathbf{F}'^{\pm}$ forms) of the wave equations look somewhat different.

As an example, here are the full first-order wave equations for the $\mathbf{F}^{\pm}, F^{\circ}$ form, which is conceptually closest to the UPPE (unidirectional pulse propagation equation) of Kolesik *et al.* [2,3] based on projections of D–

$$\nabla \times \mathbf{F}^{\pm} = \mp \imath\omega\alpha_r\beta_r \mathbf{u} \times \mathbf{F}^{\pm} \mp \frac{\imath\omega\alpha_r\beta_c}{2}\mathbf{u} \times [\mathbf{F}^+ + \mathbf{F}^-] - \frac{\imath\omega\alpha_c\beta_r}{2}\mathbf{u} \times [\mathbf{F}^+ - \mathbf{F}^-] \pm \mathbf{u} \times (\beta_r + \beta_c)\mathbf{J}, \quad (51)$$

$$\pm \nabla F^{\circ} = + \imath\omega\alpha_r\beta_r \mathbf{u} F^{\circ} + \imath\omega\alpha_c\beta_r \mathbf{u} F^{\circ}, \quad (52)$$

$$\nabla \cdot (\mathbf{F}^+ - \mathbf{F}^-) = -\imath\omega\alpha_r(\beta_r + \beta_c)\mathbf{u} \cdot (\mathbf{F}^+ + \mathbf{F}^-) + (\beta_r + \beta_c)\mathbf{u} \cdot \mathbf{J}. \quad (53)$$

VIII. CONCLUSIONS

We have introduced generalized forms of the directional field variables first envisaged by Fleck [1]. We have demonstrated that they are associated with energy fluxes in the forward and backward directions. They provide the ideal basis for the standard "forward-only" pulse propagation model, both improving our insight into pulse propagation, and allowing the backward-propagating component to be efficiently discarded if desired. By developing the theory in frequency space, we have shown how the dispersive properties of the propagation medium can be incorporated.

We have derived first-order wave equations for $\mathbf{G}^{\pm}$ that are equivalent to Maxwell's equations. If dispersion is included carefully, the equations decouple and we can get a single equation for forward-only propagation, and hence achieve significant speed gains over direct Maxwell's equation solvers for E and H (such as PSSD [5] or FDTD [6]). We have also presented a number of simulations demonstrating their use.

Since the $\mathbf{G}^{\pm}$ variables are not restricted to use in first-order wave equations, we have also presented an envelope theory and a second-order wave equation analogous to those regularly used in pulse propagation work. Either of these equations can be used to extend the practical applications of $\mathbf{G}^{\pm}$ variables into the long-pulse narrow-band regimes. Further, $\mathbf{G}^{\pm}$ can still be constructed from the E and H field obtained in traditional simulations, enabling their use for either diagnosis or analysis.

ACKNOWLEDGMENT

We would like to acknowledge useful discussions with J.C.A. Tyrrell.

[1] J. A. Fleck, Phys. Rev. B **1**, 84 (1970). Note that we use an alternative notation to avoid possible confusion with the electric field variables E (since Fleck used $E^{\pm}$, not $G^{\pm}$).
[2] M. Kolesik, J. V. Moloney, and M. Mlejnek, Phys. Rev. Lett. **89**, 283902 (2002).
[3] M. Kolesik and J. V. Moloney, Phys. Rev. E **70**, 036604 (2004).
[4] A. Ferrando, M. Zacarés, P. F. de Córdoba, D. Binosi, and Á. Montero, Phys. Rev. E **71**, 016601 (2005).
[5] J. C. A. Tyrrell, P. Kinsler, and G. H. C. New, J. Mod. Opt. **52**, 973 (2005).
[6] K. S. Yee, IEEE Trans. Antennas Propag. **AP-14**, 302 (1966).
[7] R. M. Joseph and A. Taflove, IEEE Trans. Antennas Propag. **45**, 364 (1997).
[8] A. Lakhtakia, Int. J. Infrared Millim. Waves **15**, 369 (1994).
[9] P. Hillion, J. Phys. A **28**, 2647 (1995).
[10] H. E. Moses, SIAM J. Appl. Math. **21**, 114 (1971).
[11] T. Brabec and F. Krausz, Phys. Rev. Lett. **78**, 3282 (1997).
[12] P. Kinsler, and G. H. C. New, Phys. Rev. A **67**, 023813 (2003).
[13] B. Fornberg, *A Practical Guide to Pseudospectral Methods* (Cambridge University Press, Cambridge, 1996).
[14] A. Taflove and S. C. Hagness, *Computational Electrodynamics: the Finite-Difference Time-Domain Method* (Artech House, Boston, 2000).
[15] P. Kinsler, J. C. A. Tyrrell, S. B. P. Radnor, and G. H. C. New (unpublished).
[16] P. Kinsler, arXiv.org/physics/0212014
[17] P. Kinsler, to be submitted to arXiv.org/physics.